Rime Ice Occurrences from Radiation Fog that Impact Overhead Transmission Lines in Central Washington State

Ronald M. Thorkildson[1]

[1] *Sisters, Oregon, U.S.A.*

rthorkildson@bendbroadband.com

Abstract— **Accretions of rime ice caused by freezing radiation fog can sometimes become great enough to damage overhead power lines in the Columbia Basin of Washington State. A number of these are high voltage transmission lines, owned and operated by the Bonneville Power Administration (BPA), that have long histories of outages associated with the occurrence of rime ice. This paper discusses many of the meteorological factors that make this region so rime ice-prone. It further attempts to explain why the most damaging icing events tend to occur at elevated, highly exposed locations within the basin where accretions of ice appear to have been enhanced. A detailed examination of one such icing episode is offered to demonstrate the methodology used in identifying the underlying cause of the damage to 11 lattice steel transmission towers. It is also suggested that on-line weather forecasting models might be useful in assessing the likelihood of the formation of radiation fog.**

Keywords— ***rime ice, radiation fog, adiabatic cooling, cold air pooling, transmission lines***

I. Introduction

Loads on exposed structures imposed by atmospheric icing are a well-known phenomenon. Precipitation ice, such as glaze ice caused by freezing rain or drizzle, or accretions of wet snow, are common wintertime occurrences in many parts of the world. Likewise, deposits of rime ice from non-precipitation processes, e.g. in-cloud icing, can result in severe ice loads when combined with strong winds in mountainous regions where cloud bases are lower than the terrain height [1]. While hoarfrost is also a non-precipitation form of ice, it rarely, if ever, results in meaningful ice loads. Substantial rime icing can also occur in locales prone to radiation fog at sub-freezing air temperatures when conditions favorable for its formation persist long enough. One such area in the United States is in the states of central Washington and extreme north central Oregon.

In 2009 a paper entitled "In-cloud Icing in the Columbia Basin" was published in *Monthly Weather Review*, a journal of the American Meteorological Society [2]. In that paper authors Thorkildson, Jones and Emery detailed an icing episode that seriously damaged a high-voltage transmission line located in the western portion of the Columbia Basin. An abbreviated description of this event is offered as a typical example of rime icing in the basin.

A further objective of this paper is to show that not all power lines in the basin are equally at risk for damaging rime ice, and that elevation and exposure to even light winds can significantly enhance ice accretions.

Finally, it will be shown how on-line weather products can be used as guidelines to help forecast the onset and duration of rime icing occurrences.

II. Background

Created by an act of Congress in 1937, the Bonneville Power Administration (BPA) is an agency of the United States government responsible for marketing and distributing electrical power throughout the Pacific Northwest. The power is generated by 31 federal hydroelectric dams and several small nonfederal power plants operated by the U.S. Army Corps of Engineers and the Bureau of Reclamation. These dams are located primarily on the Columbia and Snake Rivers.

Several of BPA's high-voltage transmission lines that carry electrical power from the generating sites to the load centers pass through the Columbia Basin. Some of these lines have lengthy histories of outages that have been correlated to the presence of rime ice. One such episode will serve as a case study in Section IV.

III. Meteorology

A. *Rime Ice Formation*

The Columbia Basin is a shallow bowl-shaped semi-arid region in central Washington, extending southward into extreme north central Oregon, that lies in the rain shadow of the Cascade Mountain Range. This area spans more than 225,330 km^2 and is characterized by steep river canyons, extensive plateaus and, in places, tall sinuous ridges (Fig. 1).

During the winter months the basin is susceptible to cold-air pooling [3] [4]. The low-lying topography tends to confine cold air that develops when high pressure systems build into the Pacific Northwest producing conditions favorable for nighttime radiational cooling. The loss of heat from the earth's surface is maximized when skies remain clear with little or no surface wind. Often accompanied by moderate-to-strong ridging aloft, these anticyclonic circulations result in dry, stable conditions, diverting the normally frequent progression of Pacific storms northward into British Columbia and southeastern Alaska. If this kind of pattern persists long enough, strong inversions can develop as surface temperatures drop due to the longer nights of winter.

What happens next depends upon how much water vapor is in the air. If an arctic air mass from Canada moves southward and settles into the region, it will typically be cold and very dry, possessing a low dew-point temperature. In this

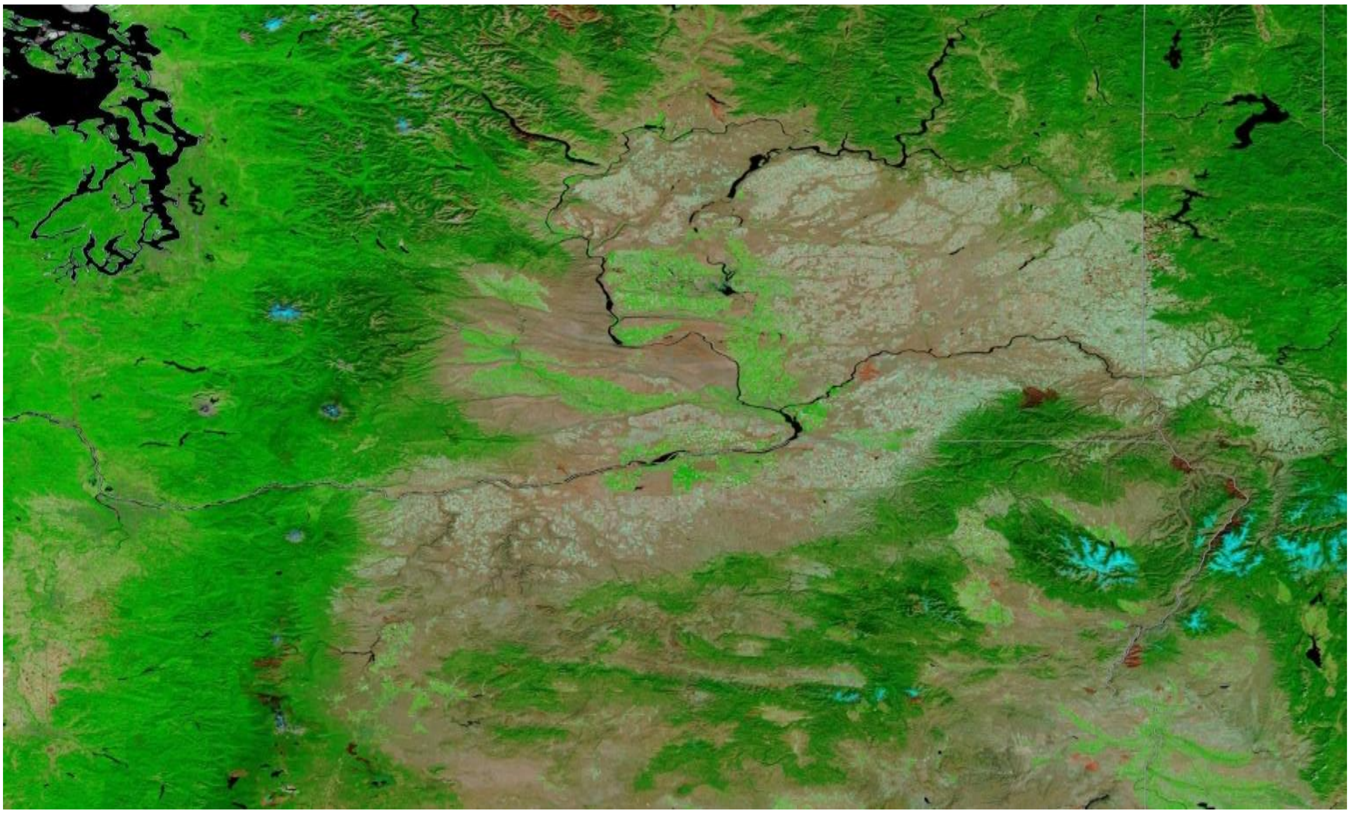

Fig. 1 The Columbia Basin of Washington State encompasses more than 225,330 km^2 in area.

instance, no matter how long the radiational cooling persists, it is unlikely the air temperature will chill to the dew-point temperature though skies remain clear throughout the period.

What more frequently takes place, however, is that a maritime polar air mass will move in behind a Pacific cold front just ahead of the building high pressure system. In this case clear skies and light winds will still promote strong radiational cooling but maritime air normally carries more water vapor, thus has a higher dew-point temperature. If the stable weather pattern holds long enough, the stagnant air nearest the ground will eventually reach saturation. Once fog forms, further radiational cooling is severely limited because the water droplets absorb much of the heat from the ground and re-radiate it in all directions. If the temperature of the air falls below freezing, the droplets of fog become supercooled (remain in a liquid state) since they tend to glaciate only at very low temperatures. With the addition of even light winds, conditions are now ripe for the accretion of rime ice.

B. *Rime Ice Enhancement*

The outages that occur in the basin due to rime icing are strongly correlated with exposure and elevation. Portions of transmission lines that run along the top of ridges or escarpments, or even atop modest hills are particularly susceptible to rime ice enhancement. Initially when a strong high pressure system settles over an area, surface winds tend to be very light or non-existent, producing optimum conditions for cold air pooling. But over time uneven cooling on the meso- and micro- scales, or even macro shifts in the weather pattern, such as the approach of a front near the end of an extended icing event, can result in horizontal pressure gradients sufficient to get the dense air moving. As the advected air encounters an elevated terrain feature, it is forced to rise and further cool due to adiabatic expansion. If air at the lower elevation is already saturated, or nearly so, additional condensed moisture will be released as the air rises, producing a cloud that often shrouds the elevated feature.

C. *Cloud Liquid Water Content*

The approach used in this section to quantify the additional moisture released into the lifted air using equations 1-10 is explained and referenced in the Thorkildson et al paper. In addition, formula (5) corrects a typo in that paper. This formulation requires basic weather data, including air temperature, dew-point temperature and barometric pressure from a low-elevation weather station upwind of a terrain feature.

Using the air temperature and dew-point temperature, the temperature of the cloud base T_c can be calculated iteratively from

$$\frac{T_c}{T_1} \approx \left(\frac{e_s\left(T_c\right)}{e_s\left(T_{d1}\right)} \right)^k \tag{1}$$

where k=0.286. T_1 (^{o}C) and T_{d1} (^{o}C) are the air temperature and dew point temperature at the valley weather station at elevation z_1. The saturation vapor pressure over water is given by

$$e_s\left(T\right) = 6.112 e^{\frac{17.67T}{T+243.5}} \tag{2}$$

Once the temperature at the base of the cloud that is created by the forced vertical motion of the near-saturated air is known, the cloud base elevation z_c is determined from

$$z_c = z_1 + \frac{T_1 - T_c}{\gamma_d} \quad (3)$$

where γ_d =0.0098°C m^{-1} is the dry adiabatic lapse rate. The temperature at elevation z within the cloud is then

$$T(z) = T_1 - \gamma_d (z_c - z_1) - \gamma_w (z - z_c) \quad (4)$$

The moist adiabatic lapse rate within the cloud is given by

$$\gamma_w = \gamma_d \frac{1 + \frac{Lw}{RT}}{1 + \frac{L^2 \varepsilon w}{R c_p T^2}}, \quad (5)$$

where

ε is the ratio of the molecular weights of water vapor and dry air (0.622), L is the latent heat of vaporization of water (2.501x10^{6} J kg^{-1}), R is the gas constant for dry air (287 J kg^{-1} K^{-1}), and c_p is the heat capacity of moist air ≈ [1005(1+0.8w) J kg^{-1} K^{-1}].

It should be noted that we are free to ignore the actual environmental lapse rate because of our assumption that the cloud is created by air forced to rise over an elevated terrain feature. Therefore, the calculation of the cloud base temperature and the temperature profile in the cloud are based solely on the dry and most adiabatic lapse rates.

The mixing ratio w, the mass of water vapor per mass of dry air, is related to the saturation vapor pressure

$$w = \varepsilon \frac{e_s}{p}. \quad (6)$$

It is used here because mixing ratios remain constant during a dry adiabatic process without entrainment. Therefore, the mixing ratio at a valley weather station,

$$w(z_1) = \varepsilon \frac{e_s(T_{d1})}{p_1} \quad (7)$$

is equal to the mixing ratio at the cloud base. The difference between $w(z_1)$ and the reduced mixing ratio at some level z above the cloud base is the cloud liquid water mixing ratio. Finally, the cloud liquid water content $W(z)$ is calculated from

$$W(z) = \left(w(z_1) - \varepsilon \frac{e_s(T(z))}{p(z)} \right) \rho(z), \quad (8)$$

where ρ(z) and p(z) are the density of dry air and the air pressure at elevation z. Pressure is calculated from the measured pressure p_1 at z_1 using

$$p(z) = p_1 \left(1 - \frac{\gamma_e (z - z_1)}{T_1 + 273.15} \right)^{\frac{g}{\gamma_e R}} \quad (9)$$

where g=9.8 m s^{-2}, and γ_e=0.0065°C m^{-1} is the standard environmental lapse rate. The density of dry air is calculated from the air pressure

$$\rho = \frac{0.348 x 10^{-3} p}{T + 273.15} \quad (10)$$

Although this establishes a method for calculating the additional water content of the lifted air, the extra amount of accreted ice that results depends on many factors. Among these are droplet concentration (or drop diameter) and wind speed.

IV. Case Study

A. *Line Failure*

On the morning of 24 November 2005 a high-voltage transmission line owned and operated by BPA experienced an outage that shut down the line. The interruption was located in a section of the line that runs along the edge of an escarpment approximately 16 km north of Wenatchee, Washington. Later that same day a transmission line maintenance crew arrived on the scene to discover that the tops of 11 lattice steel suspension towers had collapsed longitudinally (Fig. 2). At the time of the visit the temperature was sub-freezing, with fog and little, if any, wind. Both the conductor and overhead ground wire were covered with rime ice (Fig. 3).

A week later an engineering meteorologist and a team of structural engineers visited the site in an attempt to determine what led to the failure. An inspection of the crumpled tower steel showed no obvious signs of excessive corrosion, wear, or fatigue. The low-density rime ice that remained on the conductor and ground wire was found on the west side, indicating 1) that the ice formed from supercooled cloud droplets rather than freezing rain or drizzle, and 2) that winds during the in-cloud icing event had a westerly component. Three chunks of ice that fell from the conductors or ground wires (presumably when the tower tops failed) were found in the snow below. One sample (Fig. 4)

Fig. 2 An example of one of the 11 failed towers on the exposed escarpment near Wenatchee.

Fig. 3 A section of iced ground wire lies on the ground.

that was measured and weighed had a cross-sectional area of 52 cm^2 and density of 0.2 g cm^{-3}.

The following is a description of the weather conditions that preceded the failure. On 14 November 2005, maritime polar air settled into the Pacific Northwest behind a Pacific cold front (Fig. 5a). Forty–two hours later a surface high pressure system built into the region that would last for several days (Fig. 5b). Initially, this resulted in clearing skies, allowing nighttime radiational cooling to occur. By 19 November a strong ridge of warm air aloft became established (Fig. 5c) that capped an inversion that persisted for several days. Eventually, the air temperature chilled to the dew-point temperature and the basin began to fill with fog and low clouds (Fig. 6). The transmission line failure would occur five days later.

Fig. 4 A sample of rime ice presumed to have fallen from the ground wire was recovered and its density measured.

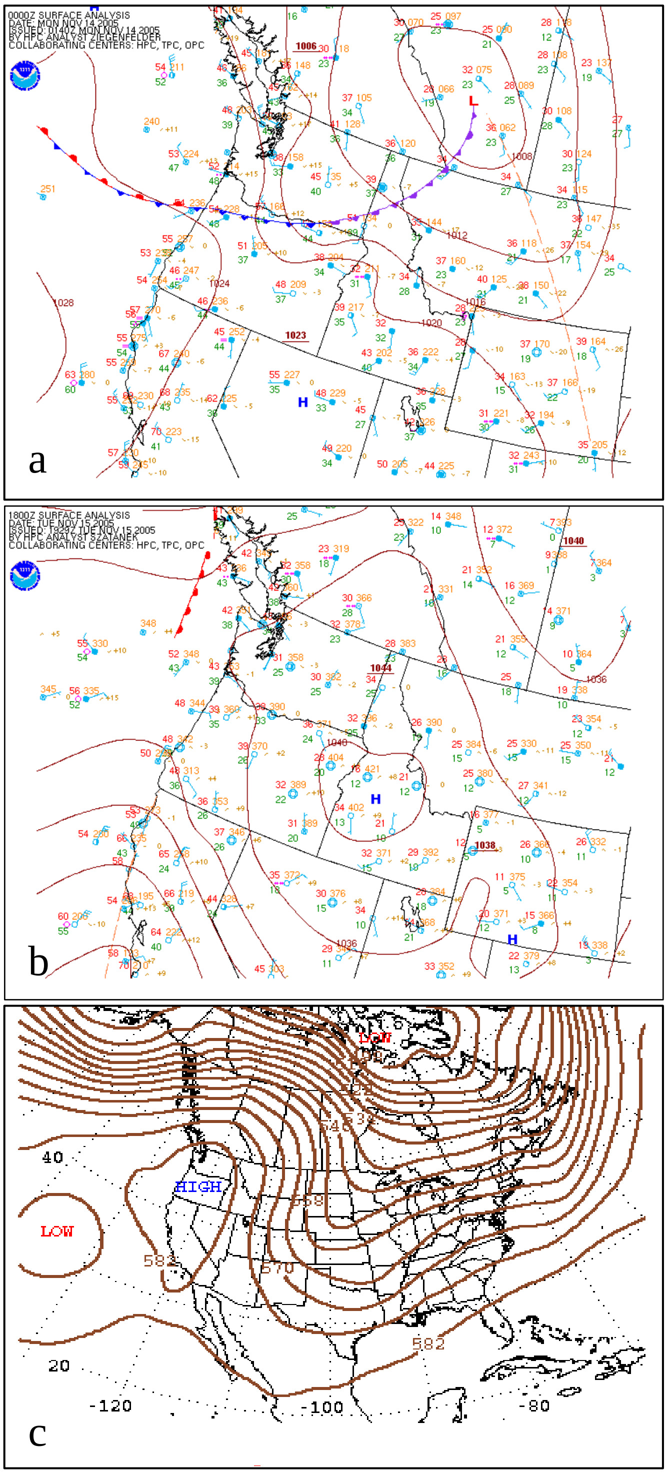

Fig. 5 Surface weather map for (a) 0000 UTC 14 Nov 2005, (b) 1800 UTC 15 Nov 2005, and (c) 500-mb height contours for 1200 UTC 19 Nov 2005.

B. Detailed Investigation

The results of a comprehensive examination of the line failure found in [2] are summarized here. The tops of 11 lattice steel suspension towers that collapsed longitudinally toward the south were in a section of the line that is oriented approximately N-S along an escarpment that drops off precipitously to the west toward the Columbia River (Fig. 7). Available weather data were obtained from the Automated Surface Observing System (ASOS) station at Wenatchee, a Washington Department of Transportation station at Waterville, and a Remote Automated Weather Station (RAWS) station near Douglas. Wenatchee is located about 16 km south of the affected line, while Waterville and Douglas lie 11 km and 38 km, respectively, to the northeast.

The attachment elevation of the conductor on the highest affected tower is 1,312 m; 1,177 m on the lowest tower. Elevations at Douglas, Waterville and Wenatchee are 771 m, 658 m and 375 m, respectively. Cloud liquid water contents at the maximum and minimum conductor attachment elevation were estimated using the equations in section 3c, using barometric pressure, air temperature and dew-point temperature data at Wenatchee. The base of the overcast measured at Wenatchee was well below the conductor elevations on the bluff, indicating the conductors and ground wires may have been in a subfreezing cloud for approximately five days.

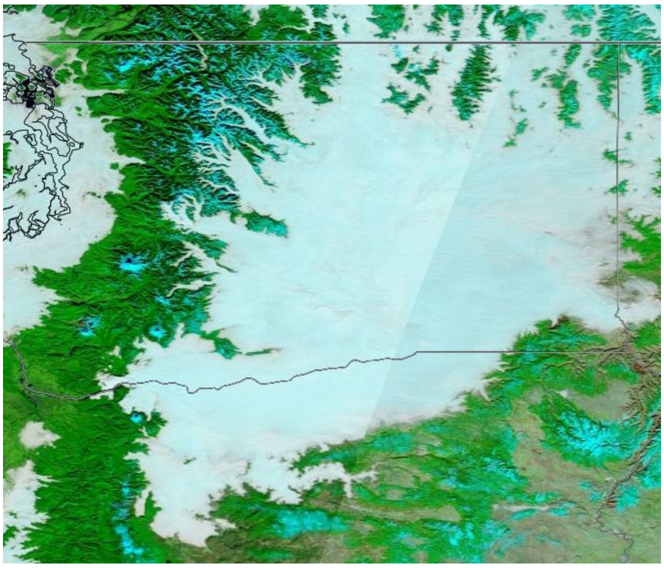

Fig. 6 Columbia Basin filled with fog and low clouds on 19 Nov 2005.

From 18 November through 24 November, temperatures at Wenatchee were above freezing, while at Waterville and Douglas they were subfreezing. Measured wind speeds at Waterville, Douglas, Wenatchee and six other ASOS stations in the basin were uniformly low throughout the period. The gridded North American Regional Reanalysis data also showed low winds that never exceeded 4 m s^{-1}. For all seven ASOS stations in the basin the wind direction tended to be from the northwest through the icing period. Though all measured wind speeds in the basin were exceedingly low, the high degree of exposure to northwesterly winds along the escarpment likely resulted in higher winds. Because of this, three scenarios for winds speeds were investigated: 1) wind speeds from the Wenatchee ASOS, but set to 1 m s^{-1} when measured speeds were zero, 2) a 5 m s^{-1} constant wind speed, 3) a 10 m s^{-1} constant wind speed. In addition, three assumptions for droplet concentrations were made, namely 175, 373 and 732 cm^{-3}. Ice loads and ice densities were calculated for the upper and lower attachment elevations of the conductor and ground wire. The conductor is a twin ACSR Chukar with a diameter of 4.1 cm, while the diameter of the ground wire is 1.3 cm. Because the conductor pairs are bound together in each span by spacers they are not free to rotate as ice freezes on the windward side of the wire. As a result the collision efficiency of the cloud droplets does not decrease as ice accretes. The ground wire, however, is free to undergo torsional rotation as the ice accretion shape changes along the span, reducing the collision efficiency.

The results of the analysis in [2] indicated that using a 5 m s^{-1} wind speed and a droplet concentration of 373 cm^{-3} provided a reasonably good explanation for the cause of the outage. It is thought that a longitudinal unbalanced ice load developed across the highest tower where the failure started, produced by a radial ice thickness of 25 mm to the north of this tower and 38 mm to the south, corresponding to loads of 0.8 and 1.5 kg m^{-1}, respectively, on the ground wire. Using these loads, BPA was able to simulate the damage to the towers on the bluff. Another piece of confirming evidence that this is the correct scenario is that the modeled ice density for a freely rotating ground wire was 0.18 g cm^{-3}, virtually the same value that was determined for the ice sample recovered at the site a week after the line outage.

C. *Another Approach*

The assumed droplet concentrations in the Columbia Basin were derived from data collected in super cooled clouds at the summit of Mt. Washington in New Hampshire. The average median volume droplet diameter d_{MVD} at Mt. Washington is about 14 µm. But it is likely that the high wind and low temperature environment on Mt. Washington is not representative of supercooled low clouds/fog in the Columbia Basin, that occur with lower wind speeds and warmer temperatures.

An approach to calculating d_{MVD} from wind speed and temperature is offered in [5].

$$d_{MVD} = -0.63 + \frac{24.56}{\sqrt{U}} + 12.418 e^{T/19.9} \qquad (11)$$

Here *U* is the wind speed and *T* is the air temperature.

We can now use d_{MVD} from (11) to calculate droplet concentrations from liquid water content

$$n_{MVD} = \frac{6W}{\pi \rho_w d_{MVD}^3} \qquad (12)$$

where n_{MVD} is the droplet concentration (cm^3) and ρ_w is the density of water.

Using this approach for the icing event in the Columbia Basin, the calculated d_{MVD} for the assumed wind speeds of 5 m s^{-1} and 10 m s^{-1} were 20 and 17 µm, respectively, for both the upper and lower wire attachment elevations. For the lower wind data from the ASOS station at Wenatchee; that d_{MVD} = 30 µm, about twice the size of droplets at Mt. Washington. Median values for the droplet concentrations were 193 and 322 cm^3 for the 5 and 10 m s^{-1} wind speeds, respectively, for the upper attachment elevation; 144 and 239 cm^3 for the lower attachment elevation. For the lowest wind speed case using ASOS data, the mean wind speed for the period was 1.6 m s^{-1}, droplet concentrations were 62 and 47 cm^3 for upper and lower elevations, respectively. These concentrations are far smaller than the concentrations assumed based on typical conditions at Mt. Washington. Because the larger drop diameters lead to higher collision efficiencies, it is reasonable to suppose that the accreted ice that caused the ground wire supports to fail may have resulted from lower wind speeds, say between 1 and 5 m s^{-1}.

V. PREDICTING THE FORMATION AND DURATION OF RADIATION FOG

The formation of radiative fog is a complex process that makes it difficult to model and to forecast [6]. The following conditions, some of which were alluded to in section 3a, are considered of primary importance in the formation of radiation fog: 1) clear nighttime skies, 2) moist air (narrow dew-point depression) in the lowest 100 meters, 3) moist

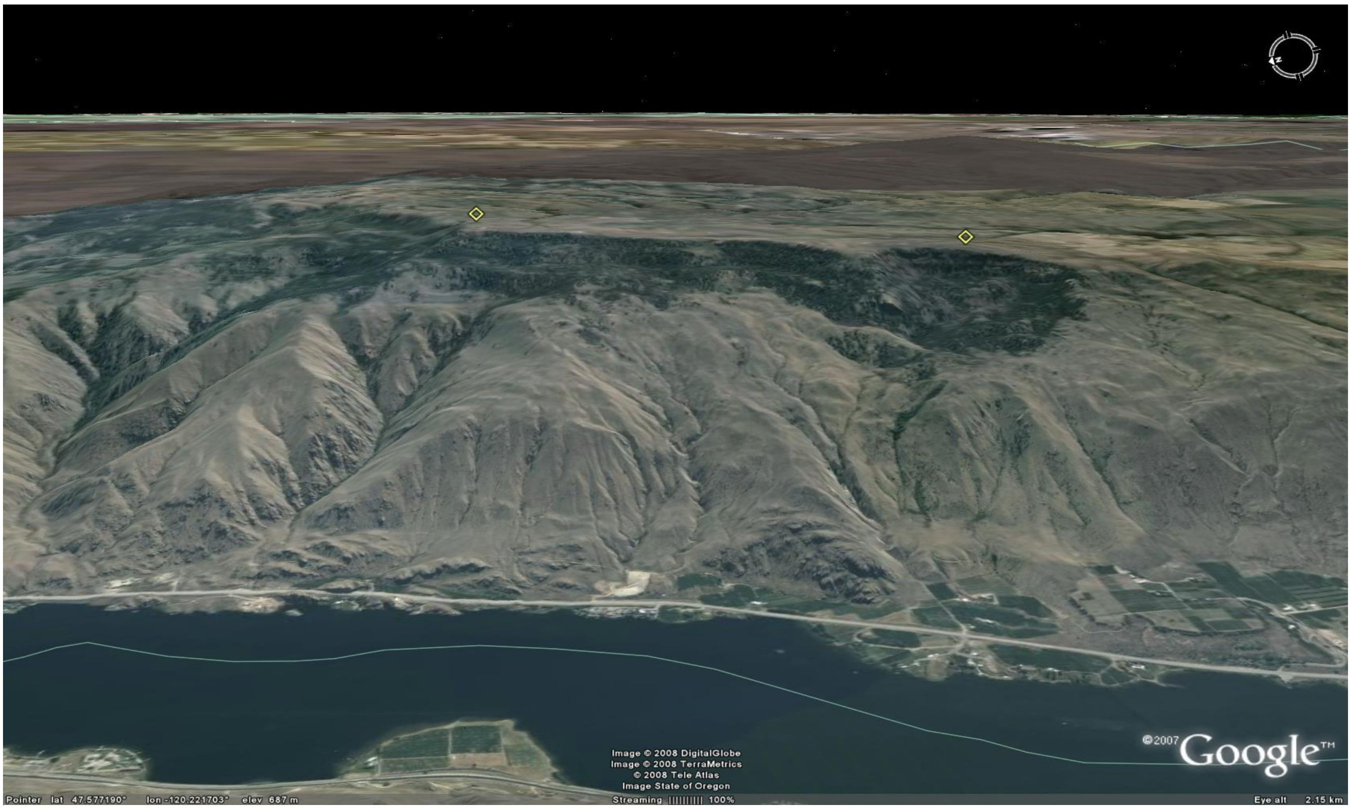

Fig 7 A view from the west of the bluff above the Columbia River. The 11 failed towers were all between the yellow diamonds.

ground, 4) weak pressure gradient and 5) favorable local topography [7]. The goal of this section is not to try to predict the onset of radiation fog per se, but to identify on-line meteorological tools to help assess the likelihood of its formation and for how long a period it might persist.

The two most widely used forecasting models are the Global Forecasting System (GFS) and the European Centre for Medium-Range Weather Forecasts (ECMWF). Either can be used equally well for this purpose. While both these models have an overwhelming suite of graphs and charts, the two most useful synoptic tools are the surface chart and the 500 mb upper air chart.

The surface chart consists of isobars (lines of equal pressure) and fronts that show boundaries between air masses of different temperatures and moisture contents at mean sea level. In the Northern Hemisphere, winds circulate counterclockwise about a low pressure center, clockwise around centers of high pressure systems. When isobars are close together wind speeds are higher, lower when they are farther apart.

The 500 mb constant pressure level is an upper air chart that most accurately depicts the locations of ridges, troughs and the winds aloft that “steer” extratropical surface storms. It consists of contour lines that connect points of equal heights above mean sea level where the atmospheric pressure is 500 mb. Because cold air is dense, a vertical column of this air at 500 mb will be shorter than a column of warmer air at the same pressure. On this chart the coldest air is found in troughs or closed lows, while the warmest air exists in the ridges.

Someone who is concerned about the possibility of radiation fog forming in a particular area need not monitor these charts continuously. When an active weather pattern is producing frequent episodes of precipitation, the presence of clouds strongly inhibits nighttime radiation cooling. But when increasing periods of clearing begin to appear, check the surface chart for the moisture content of the air (dew-point depression) and the formation of a high pressure system. Then reference the 500 mb chart to see if a ridge is moving into the area that might result in an inversion. The strongest signal for the formation of radiation fog is surface pressure high enough to keep the nighttime skies clear, overlaid by the a strong quasi-stationary ridge to cap an inversion and keep storms well away for at least three or four days. Some of this weather information may be available through the local media. Satellite images may also be useful in detecting the presence of fog.

In January 2009, using these forecasting tools, the author alerted BPA that weather conditions favorable for the formation of radiation fog were developing in the Basin. Two days later the first of two outages associated with rime ice damaged an insulator string and a double circuit tower arm on a line located about 48 km east southeast of Grand Coulee Dam (Figs. 8 and 9). Unlike the 2005 occurrence near Wenatchee, this event took place closer to the middle of the Basin. Pictures taken by BPA line crews showed accumulations of rime ice up to 25 cm thick on conductors and ground wires.

VI. CONCLUSIONS

Many high voltage electric power lines owned and operated by BPA pass through the Columbia Basin of central Washington State. Some of these lines have lengthy histories of outages that have been correlated to the presence of rime ice. A few of the icing episodes have severely damaged towers and overhead wires. One such event was described in this paper to demonstrate the kind of damage that can result and to help explain why this region is so rime ice-prone.

The shallow, bowl-like shape of the basin makes it particularly susceptible to cold air pooling. During the long, clear nights of winter the ground can cool quickly due to the loss of heat into space. As this process continues, the reservoir of cold air deepens. If the air chills to the dew-point temperature, fog will form.

Fig. 8 A January 2009 rime icing event in the central Columbia Basin that damaged a high voltage line.

It is presumed that the formation of rime ice from subfreezing radiation fog as laid out in this paper should be applicable to other temperate regions of the world where winter nights are sufficiently long to effectively chill the air within topographies that would result in cold air pooling.

Many of the events causing damage to lines occurred at elevated, highly exposed locations within the Basin. If a strong enough horizontal pressure gradient develops, air may be advected, then forced to rise, over an elevated terrain feature. Cooling already saturated air adiabatically will release additional liquid moisture into the air as it ascends. If temperatures are subfreezing, this added moisture will result in additional accreted ice. In the detailed analysis of the 2005 event, modeled temperatures along with wind speed scenarios, allowed the calculation of d_{MVDs} and drop concentrations that are more realistic than assumed in [2], indicating that relatively low wind speeds led to the unbalanced ice loads and tower failures on the bluff above Wenatchee.

Fig. 9 An overhead fibre optic cable accreted an impressive amount of rime ice during the January 2009 event.

Finally, a method of assessing the likelihood of the formation of radiation fog using weather forecasting models was offered.

Acknowledgment

The author wishes to gratefully acknowledge Kathleen Jones of CRREL for her expert advice and careful review of this paper.

References

[1] Ducloux, H., B.E.K. Nygaard (2018) Ice loads on overhead lines due to freezing radiation fog events in plains, *Cold Regions Science and Technology* 153 120-129.

[2] Thorkildson, R.M., K.F. Jones, and M.K. Emery (2009) In-cloud icing in the Columbia Basin. *Monthly Weather Review*, 137, 4369–4381.

[3] Whiteman, C. D., S. Zhong, W. J. Shaw, J. M. Hubbe, X. Bian, and J. Mittelstadt, 2001: Cold pools in the Columbia Basin, *Weather and Forecasting*, 16, 432-447.

[4] Zhong, S., C. D. Whiteman, X. Bian, W. J. Shaw, and J. M. Hubbe, 2001: Meteorological processes affecting the evolution of a wintertime cold air pool in the Columbia Basin, *Monthly Weather Review*, **129**, 2600-2613.

[5] Jones, K.F., R.M. Thorkildson, J.B. Eylander (2017) Median volume drop diameter for in cloud icing simulations, *IWAIS proceedings*, paper B2-3.

[6] Menut, L., S. Mailler, J.C. Dupont, M. Haeffelin, T. Elias (2014) Predictability of the meteorological conditions favourable to radiative fog formation during the 2011 ParisFog campaign, Bound lay Meteorol 150 (2), 277-297.

[7] Dejmal, K., V. Repal Forecasting the formation of radiation fog, Department of military geography and meteorology university of defence kounicova 65, 662 10 Brno Czech Republic.